Factors that Contribute to Efficient Catalytic Activity of a Small Ca^{2+}-Dependent Deoxyribozyme in Relation to Its RNA Cleavage Function†

Yasuhide Okumoto,‡ Yoshiatsu Tanabe,‡ and Naoki Sugimoto*,‡,§

Department of Chemistry, Faculty of Science and Engineering, and High Technology Research Center, Konan University, 8-9-1 Okamoto, Higashinada-ku, Kobe 658-8501, Japan

Received May 16, 2002; Revised Manuscript Received December 3, 2002

ABSTRACT: Recently, we found a small Ca^{2+}-dependent deoxyribozyme (unmodified), d(GCCTGGCAG$_1$G$_2$C$_3$-T$_4$A$_5$C$_6$A$_7$A$_8$C$_9$G$_{10}$A$_{11}$GTCCCT), with cleavage activity for its RNA substrate, r(AGGGACA↓UGCCAGGC) (↓ denotes the RNA cleavage site), in the presence of Ca^{2+} and developed a functional SPR sensor chip with this deoxyribozyme [Okumoto, Y., Ohmichi, T., and Sugimoto, N. (2002) *Biochemistry 41*, 2769−2773]. In the study presented here, to clarify the factors contributing to the efficient catalytic activity of the unmodified deoxyribozyme, RNA cleavage reactions were carried out using 24 mutant deoxyribozymes containing one unnatural DNA nucleotide, such as dI (2′-deoxyinosine), 7-deaza-dG, 2-aminopurine, 7-deaza-dA, 2-amino-dA, dm^{5}C (5-methyl-2′-deoxycytosine), or d^{P}C (5-propynyl-2′-deoxycytosine). The K_m values (Michaelis constants) with the mutants that lacked N7 and O6 of G$_1$ and O6 of G$_2$ were 4.5 and 6.6 times that of the unmodified one, respectively. The k_{cat} value (cleavage rate constant) with the mutants that lacked O6 of G$_{10}$ was 0.025 times that of the unmodified one. The results of UV melting curves, SPR kinetics, and CD spectra supported the quantitative idea that the catalytic activity of the unmodified form was achieved using Ca^{2+}. On the basis of these results, a preliminary model for two G$_1$·A$_8$ and G$_2$·A$_7$ mismatched base pairs such as G(*anti*)·A(*anti*) formed in the catalytic loop is proposed. The factor of 10 increase in the k_{cat}/K_m value of the mutant deoxyribozyme, which has C$_9$ substituted with d^{P}C, suggests that the base stacking interaction between the substituted propynyl group in dC and the nearest-neighbor base grew stronger. Thus, substituting d^{P}C for dC in the catalytic loop would be one of the best ways to increase the catalytic activity of the deoxyribozyme.

Much like a protein, ribozymes need to fold into an active structure, the native state, to acquire biological function. Unlike the protein folding problem, however, the question of how an RNA sequence specifies a unique fold has only recently attracted an increasing amount of attention (*1*). Recent structural studies have revealed that large RNAs often fold in a quasi-hierarchical manner (*1*). In contrast to most proteins, a change in a single RNA residue can either relieve such a kinetic folding trap (*2*) or prevent tertiary folding altogether (*3*). Convenient model systems for studying RNA folding are the ribozymes, because their catalytic function readily reports the presence of a folded native structure. The hairpin ribozyme is a small endonucleolytic RNA motif that has proven to be both a model for RNA folding problems (*1*, *3*) and a gene therapeutic agent for targeted RNA inactivation (*1*, *4*). Ribozymes and deoxyribozymes are catalysts in biological reactions. Most ribozymes require divalent metal ions to gain high catalytic activity (*5*) through the effect of these ions as catalytic and structural cofactors in ribozyme reactions. Self-splicing group I and II introns, an RNA subunit of RNase P,[1] and hammerhead, hairpin, HDV, *Neurospora* VS, and lead-dependent ribozymes (leadzymes) are well-known as typical ribozymes (*6*−*14*). These ribozymes catalyze the formation, transfer, and hydrolysis of phosphodiester bonds in the presence of Mg^{2+} or other divalent metal ions. The hammerhead ribozyme, which is a small catalytic RNA found in satellite RNAs of certain plant viruses, uses Mn^{2+}, Ca^{2+}, Cd^{2+}, or Co^{2+} for its activity as well as Mg^{2+} (*10*, *14*). The *Tetrahymena* ribozyme uses Mg^{2+} or Mn^{2+} for its activity within many species of metal ions (*6*). In contrast, Ca^{2+} inhibits the *chemical step* of the group I intron reaction by competing with Mg^{2+} at the metal binding site (*15*). Thus, it is necessary to investigate the ribozyme−metal ion interactions to gain an understanding of the function−structure relationship of the catalytic RNAs or DNAs. In addition, a recent study showed that divalent

† This work was supported in part by Grants-in-Aid for Scientific Research from the Ministry of Education, Science, Sports and Culture, Japan and a grant from the "Research for the Future" Program of the Japan Society for the Promotion of Science.

* To whom correspondence should be addressed: High Technology Research Center, Konan University, 8-9-1 Okamoto, Higashinada-ku, Kobe 658-8501, Japan. Phone: +81-78-435-2497. Fax: +81-78-435-2539. E-mail: sugimoto@konan-u.ac.jp.

‡ Department of Chemistry, Faculty of Science and Engineering.

§ High Technology Research Center.

[1] Abbreviations: RNase, ribonuclease; HDV, hepatitis delta virus; dI, 2′-deoxyinosine; dm^{5}C, 5-methyl-2′-deoxycytosine; d^{P}C, 5-propynyl-2′-deoxycytosine; UV, ultraviolet; CD, circular dichroism; SPR, surface plasmon resonance; HPLC, high-performance liquid chromatography; TBHP, *tert*-butyl hydroperoxide; DCM, dichloromethane; MES, 2-morpholinoethanesulfonic acid; HEPES, *N*-(2-hydroxyethyl)piperazine-*N*′-2-ethanesulfonic acid; Tris, tris(hydroxymethyl)aminomethane; CHES, *N*-cyclohexyl-2-aminoethanesulfonic acid; EDTA, ethylenediaminetetraacetic acid; BIA, biomolecular interaction analysis; k_a, association rate constant; k_d, dissociation rate constant; RU, resonance units for a ligand binding to an immobilized probe; T_m, melting temperature in degrees Celsius; NMR, nuclear magnetic resonance.

10.1021/bi020364z CCC: $25.00
Published on Web 01/28/2003

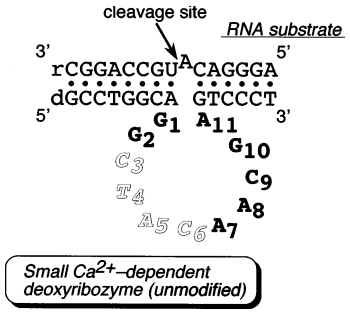

FIGURE 1: Secondary structure of the complex of the small Ca^{2+}-dependent deoxyribozyme (unmodified) and its RNA substrate. This deoxyribozyme binds its RNA substrate through two substrate recognition domains, each involving Watson−Crick base pairs. The arrow denotes its RNA cleavage site. Bold letters represent the active nucleotides in the catalytic loop. Open italic letters represent the inactive nucleotides.

ions were not necessary for RNA cleavage activity under very high concentrations of lithium or even ammonium ion with the hammerhead, hairpin, and *Neurospora* VS ribozymes (*16*−*18*). On the other hand, there are various metal-dependent deoxyribozymes (DNA enzymes) with phosphodiesterase activity in the presence of Ca^{2+}, Cu^{2+}, Mg^{2+}, Pb^{2+}, or Zn^{2+} (*19*−*23*). Although these reaction conditions are not normal physiological conditions in vivo, these results are still surprising. Therefore, we now need to reconsider the relationship between metal ions and the ribozymes and/or deoxyribozymes.

Recently, we uncovered the small Ca^{2+}-dependent deoxyribozyme (unmodified), d(GCCTGGCAG$_1$G$_2$C$_3$T$_4$A$_5$C$_6$A$_7$A$_8$C$_9$G$_{10}$A$_{11}$GTCCCT), with cleavage activity for its RNA substrate, r(AGGGACA↓UGCCAGGC) (↓ denotes its RNA cleavage site; see Figure 1) (*24*, *25*). The design of this deoxyribozyme was based on the 10−23 DNA enzyme derived from the 23 round clone obtained after the 10th round of the in vitro selection procedure (*19*, *26*). This deoxyribozyme lacked four nucleotides from the catalytic loop in the 10−23 DNA enzyme that exhibited the best activity in the presence of Mn^{2+} and low activity for Mg^{2+} and Ca^{2+} (*26*). The catalytic efficiency of this deoxyribozyme in the presence of Ca^{2+} was 24 times that in the presence of Mg^{2+}, indicating that this deoxyribozyme has a different and higher metal ion selectivity than the 10−23 DNA enzyme. Compared with RNA molecules, DNA molecules have several advantageous features. DNA is also amenable to molecular design by rational and combinational methods; DNA can be easily synthesized, and DNA and *unnatural* DNA are more stable than their RNA counterparts. These intrinsic properties of DNA give the deoxyribozyme a higher potential value as a tool for therapeutic and industrial applications that are attracting considerable attention because of its small size, its strong catalytic activity in an RNA cleavage reaction, and its flexibility in the selection of a target site (*19*, *27*). An immobilized deoxyribozyme on a SPR sensor chip has become a useful tool for distinguishing RNA foldings (*28*). A clear understanding of the structure of active sites and important factors affecting the catalytic activity is necessary for designing better deoxyribozymes. The deoxyribozyme in this study is an interesting and promising catalytic oligonucleotide for understanding specific metal ion−DNA interactions.

In this study, to clarify the factors contributing to the efficient catalytic activity of the deoxyribozyme, RNA cleavage reactions were carried out using 24 mutants of the deoxyribozyme. Recently, it was shown that seven nucleotide positions in the catalytic loop of the unmodified form (G_1, G_2, A_7, A_8, C_9, G_{10}, and A_{11}) are important for the RNA cleavage activity in the presence of Ca^{2+} (*24*, *25*). Therefore, we used mutant deoxyribozymes containing one unnatural DNA nucleotide (dI, 7-deaza-dG, 2-aminopurine, 7-deaza-dA, 2-amino-dA, dm^{5}C, or d^{P}C) in these seven positions in the catalytic loop (see parts a−j of Figure 2).

EXPERIMENTAL PROCEDURES

Preparation of Oligonucleotides. All the DNA and RNA oligonucleotides were chemically synthesized on a solid support as previously described (*24*, *25*, *29*). The blocked unnatural nucleotide and biotin phosphoramidites were purchased from Glen Research Co., Ltd. (Sterling, VA). The DNA oligonucleotide containing 7-deaza-dG was oxidized using TBHP in a DCM solution (37:67, v/v) for 6 min. The DNA oligonucleotides containing 2-amino-dA or d^{P}C were deprotected by treatment with 25% ammonia at 55 °C for 24 or 12 h, respectively. The DNA and RNA oligonucleotides were purified by reverse-phase HPLC and electrophoresis on a 20% polyacrylamide (19% acrylamide and 1% bisacrylamide)/7 M urea denaturing gel. The final purity of the DNA and RNA oligonucleotides was confirmed to be >99%. All the DNA and RNA oligonucleotides were desalted through a Sep-Pak C18 cartridge column (Waters) before use. Single-strand concentrations of the purified DNA and RNA oligonucleotides were determined by measuring the absorbance at 260 or 280 nm at high temperatures. The single-strand extinction coefficients were calculated via the mononucleotide and dinucleotide using a nearest-neighbor approximation (*30*). The average values of the DNA−RNA extinction coefficients were used as extinction coefficients for the sequences containing the DNA−RNA chimera junctions.

RNA Cleavage Reactions. The RNA cleavage reactions by the deoxyribozymes were carried out under multiple-turnover conditions at 37 °C as previously described (*24*, *25*). The buffer solution contained 50 mM MES (pH 6.0−7.0), HEPES (pH 7.0−7.5), Tris (pH 7.5−9.0), or CHES (pH 9.0−10). The RNA substrate with the 5′-OH group was labeled at the 5′-end with ^{32}P (*24*, *25*). After the cleavage reactions were stopped, the 5′-end-labeled product and RNA substrate were separated by electrophoresis on 20% polyacrylamide/7 M urea denaturing gels (*24*, *25*). The RNA cleavage yields were determined by quantifying the radioactivity in the bands of the 5′-end ^{32}P-labeled products and the RNA substrate with a Bio-Image Analyzer model BAS 2000 (Fuji Photo Film, Tokyo, Japan). The k_{cat} (cleavage rate constant) and K_m (Michaelis constant) values were calculated from Eadie−Hofstee plots based on the Michaelis−Menten mechanism (*24*, *25*, *31*). To determine these values, we carried out at least three independent experiments. The estimated average errors in the k_{cat}, K_m, and k_{cat}/K_m values are ±8.3, ±6.8, and ±9.8%, respectively.

UV Melting Measurements. Melting curves (absorbance vs temperature curves) were measured at 260 nm with a Hitachi U-3210 spectrophotometer connected to a Hitachi SPR-10 thermoprogrammer as previously described (*32*). The

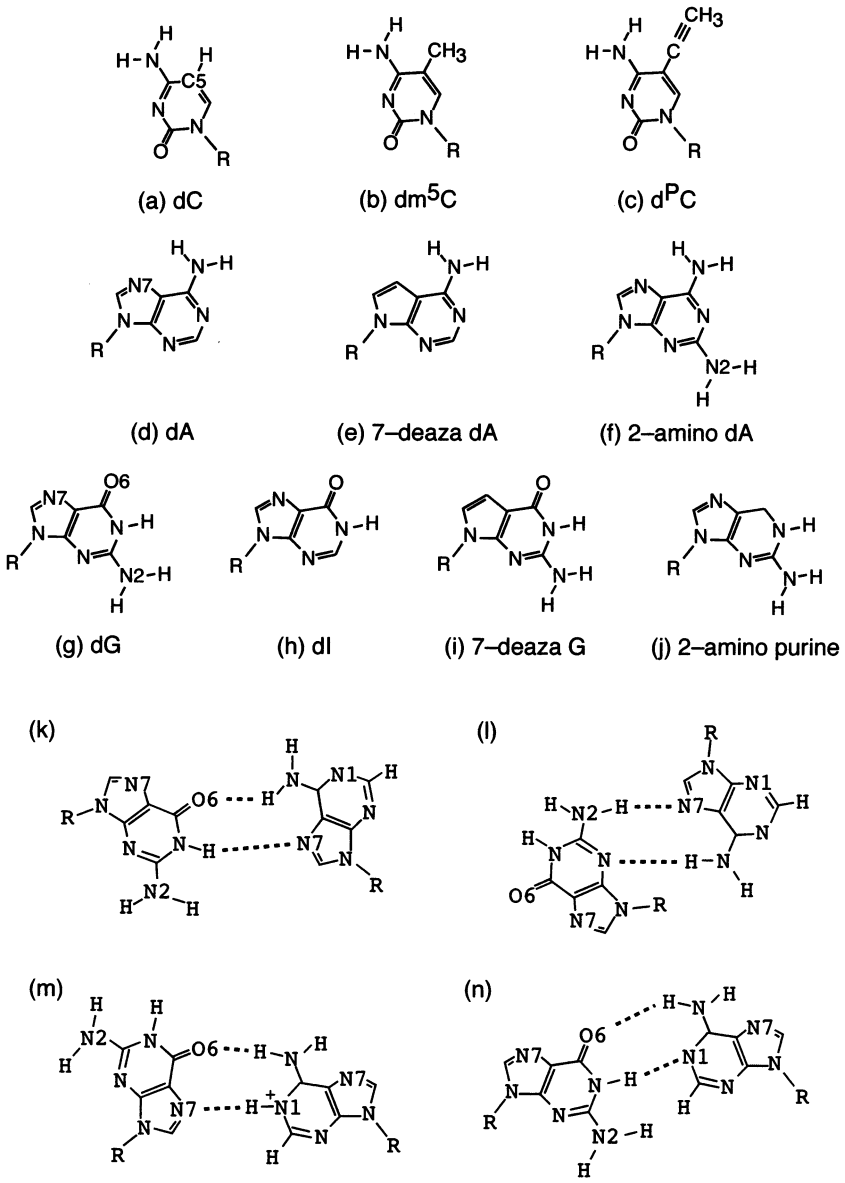

FIGURE 2: Chemical structures of the various nucleotides: (a) dC, (b) dm^{5}C, (c) d^{P}C, (d) dA, (e) 7-deaza-dA, (f) 2-amino-dA, (g) dG, (h) dI, (i) 2-aminopurine, and (j) 7-deaza-dG. Four base pairing arrangements for G·A base pairs. Dotted lines represent possible hydrogen bonding interactions. (k) The G(*anti*)·A(*syn*) base pair has two hydrogen bonds [N1(G)−N7(A) and O6(G)−N2(A)]. (l) The sheared G·A base pair has two hydrogen bonds [N2(G)−N7(A) and N3(G)−N2(A)]. (m) The G(*syn*)·A$^+$(*anti*) base pair has two hydrogen bonds [N7-(G)−N1(A) and O6(G)−N2(A)]. (n) The G(*anti*)·A(*anti*) base pair has two hydrogen bonds [N1(G)−N1(A) and O6(G)−N2(A)]. R represents a sugar.

heating rate was 0.5 °C/min in cuvettes with a path length of 0.1 cm. The buffer solution contained 50 mM Tris-HCl (pH 8.0) and 25 mM Ca^{2+}. The deoxyribozyme and its pseudo-RNA substrate [rAGGGAC(dA)UGCCAGGC] were mixed 1:1 to obtain each deoxyribozyme−pseudo-RNA substrate complex. The pseudo-RNA substrate was confirmed not to be cleaved by the deoxyribozyme in the presence of Ca^{2+}. The concentration of the oligonucleotides was 10 μM.

CD Measurements. The CD spectra were obtained using a JASCO J-600 spectrophotometer with a JASCO PTC-348 temperature controller and interfaced with a Dell OptiPlex GXi computer. All the CD spectra were measured from 340 to 200 nm in cuvettes with a path length of 0.1 cm at least in triplicate at 5 °C. The conditions were the same as those in the UV measurements.

SPR Measurements. A BIAcore (BIAcore 1000, Biacore AB, Uppsala, Sweden) was used in the SPR measurements at a flow rate of 5 μL/min in a buffer containing 50 mM Tris-HCl (pH 8.0) and 25 mM Ca^{2+} at 20 °C as previously described (*25*). The immobilized ligand was the 5′-biotinylated pseudo-RNA substrate. The level of the immobilized ligand was within the low level that must be used to ensure that the observed binding rate will be limited by the reaction kinetics rather than by the transport effect of the injected deoxyribozyme (*33*). In addition, to remove the background binding between the injected deoxyribozyme and the immobilized streptavidin to the dextran matrix or the refractive index change in the injection, the SPR trace after the buffer containing the deoxyribozyme had been allowed to flow over the sensor chip coated without the 5′-biotinylated pseudo-RNA substrate was deducted from those with it. The concentration range of the injected deoxyribozyme was from 0.1 to 400 μM. The k_a (association rate constant) and k_d (dissociation rate constant) in the complex formation of the

Table 1: Kinetic Parameters for the RNA Substrate Cleavage Reaction by the Unmodified and Mutant Deoxyribozymes and Stability of the Complex of the Deoxyribozyme and Its RNA Substrate in the Presence of Ca^{2+} [a]

deoxyribozyme	substitution	K_m (nM)	k_{cat} (min^{-1})	k_{cat}/K_m ($\times 10^{-7}$ M^{-1} min^{-1})	k_{cat}/K_m(relative)	T_m [b] (°C)
unmodified[c]	none	124 ± 3.0	2.04 ± 0.19	1.7	1.0	55.9
mutant **1**	$C_6 \rightarrow d^pC$	131 ± 8.2	1.99 ± 0.14	1.5	0.93	55.2
mutant **2**	$C_9 \rightarrow dm^5C$	79.2 ± 7.0	1.79 ± 0.13	2.3	1.4	58.8
mutant **3**	$C_9 \rightarrow d^pC$	22.8 ± 1.6	3.86 ± 0.24	17	10	65.1
mutant **4**	$A_7 \rightarrow$ 7-deaza-dA	139 ± 11	1.93 ± 0.11	1.4	0.84	54.6
mutant **5**	$A_8 \rightarrow$ 7-deaza-dA	144 ± 12	2.21 ± 0.19	1.5	0.93	54.1
mutant **6**	$A_{11} \rightarrow$ 7-deaza-dA	144 ± 11	1.94 ± 0.17	1.3	0.82	54.2
mutant **7**	$A_7 \rightarrow$ 2-amino-dA	249 ± 18	1.49 ± 0.11	0.60	0.36	51.3
mutant **8**	$A_8 \rightarrow$ 2-amino-dA	301 ± 24	1.67 ± 0.14	0.55	0.34	50.2
mutant **9**	$A_{11} \rightarrow$ 2-amino-dA	139 ± 9.2	1.79 ± 0.15	1.3	0.78	54.6
mutant **10**	$G_1 \rightarrow$ dI	130 ± 7.6	1.91 ± 0.17	1.5	0.89	55.3
mutant **11**	$G_2 \rightarrow$ dI	136 ± 8.5	2.01 ± 0.20	1.5	0.90	54.9
mutant **12**	$G_{10} \rightarrow$ dI	131 ± 6.6	1.79 ± 0.16	1.4	0.83	55.2
mutant **13**	$G_1 \rightarrow$ 7-deaza-dG	553 ± 31	1.63 ± 0.093	0.30	0.12	47.8
mutant **14**	$G_2 \rightarrow$ 7-deaza-dG	121 ± 6.8	1.89 ± 0.12	1.6	0.95	56.0
mutant **15**	$G_{10} \rightarrow$ 7-deaza-dG	127 ± 10	2.11 ± 0.20	1.7	1.0	55.6
mutant **16**	$G_1 \rightarrow$ 2-aminopurine	832 ± 57	1.55 ± 0.11	0.19	0.11	45.1
mutant **17**	$G_2 \rightarrow$ 2-aminopurine	775 ± 37	1.79 ± 0.17	0.23	0.14	46.5
mutant **18**	$G_{10} \rightarrow$ 2-aminopurine	144 ± 11	0.0512 ± 0.0047	0.035	0.021	54.2

[a] All experiments of RNA cleavage were carried out in a buffer containing 50 mM Tris-HCl (pH 8.0) and 25 mM Ca^{2+} under multiple-turnover conditions with 10−1000 nM 5′-end ^{32}P-labeled RNA substrate and 1 nM deoxyribozyme at 37 °C. [b] The T_m value was calculated at a total oligomer concentration of 10 μM. [c] Data from ref *24*.

deoxyribozyme and RNA substrate were determined using eqs 1 and 2 (*25*, *34*):

$$dRU/dt = k_a[Dz]RU_{max} - (k_a[Dz] + k_d)RU \quad (1)$$

$$k_{obs} = k_a[Dz] + k_d \quad (2)$$

where RU is a resonance unit, [Dz] is the concentration of the deoxyribozyme, RU_{max} is the maximum ligand binding capacity of the immobilized probe, and k_{obs} is the observed rate constant for formation of the deoxyribozyme−RNA substrate complex. The $\Delta G°_{20}$ values for the binding for the deoxyribozyme−RNA substrate complex were obtained from eq 3:

$$\Delta G°_{20} = -293.15R \ln(k_a/k_d) \quad (3)$$

where R is the gas constant.

RESULTS

Dependence of Catalytic Efficiencies on the Concentration of Ca^{2+} and pH. To investigate the role of the metal ions in the deoxyribozyme reactions, the RNA cleavage reactions were first carried out in various concentrations of Ca^{2+} (see Figure S1 of the Supporting Information). Additions of up to 15 mM Ca^{2+} resulted in a large decrease in K_m, and large increases in k_{cat} and k_{cat}/K_m (second-order rate constant). The addition of Ca^{2+} in excess of 15 mM resulted in no further change in the K_m, k_{cat}, and k_{cat}/K_m values. Here the total metal ion concentration was kept at 25 mM in this study. To determine that k_{cat} is mainly due to RNA cleavage, the RNA cleavage reactions were carried out at various pHs. The slope of the log(k_{cat}) versus pH plot was almost equal to 1 from pH 6.5 to 9.0, indicating that the k_{cat} value reflected the RNA cleavage (see Figure S2 of the Supporting Information). Above pH 9.0, the RNA cleavage rate was lower than that predicted from the extrapolation of rates at lower pH values, probably because of deprotonation of the nucleobase as seen in the hammerhead ribozymes (*11*, *35*, *36*).

dC Substitution. Freier and Altmann showed that substitution at the carbon 5 position of cytosine leads to stabilization of the duplex because the carbon 5 position is in the stack of the duplex (*37*). Our results also indicated that dm^5C and d^pC were useful for probing the stacking interactions with dC in the duplex region (*38*). To obtain information about the specific role of dC in the catalytic loop, RNA cleavage reactions were carried out using mutants **1**−**3** that have C_6 or C_9 substituted with dm^5C or d^pC (see Figures 1 and 2a−c and Table 1). The RNA cleavage site of these mutants was the same as that of the unmodified form and of mutants **4**−**12** as will be described later. Table 1 lists the kinetic parameters of the deoxyribozyme reactions. The K_m and k_{cat} values of mutant **1** with C_6 substituted with d^pC, a position in the catalytic loop, were very similar to those of the unmodified one (see Table 1), indicating that C_6 in the catalytic loop of the deoxyribozyme is at a position of little importance for RNA cleavage activity in the presence of Ca^{2+} (*24*). In contrast, C_9 in the loop is an important position for RNA cleavage activity (*24*). The k_{cat}/K_m value of mutant **2** was also similar to that of the unmodified one, but the k_{cat}/K_m of mutant **3** was 10 times that of the unmodified one. This increase in k_{cat}/K_m of mutant **3** depended on both the decrease in K_m and the increase in k_{cat}, indicating that the substitution of C_9 with d^pC affected both the folding and its RNA cleavage activity.

dA Substitution. A study of the hammerhead ribozyme showed that N7 of A in the catalytic loop was critical for efficient cleavage activity (*39*), suggesting a preliminary model for the binding of a metal ion cofactor to its adenine. To determine the specific role of dA in our catalytic loop, RNA cleavage reactions by mutants **4**−**9**, which have A_7, A_8, or A_{11} substituted with 7-deaza-dA or 2-amino-dA, were investigated (see Figure 2d−f and Figure S3 of the Supporting Information). The k_{cat}/K_m values for mutants **4**−**9** were similar to that of the unmodified one (see Table 1), but the k_{cat}/K_m values of mutants **7** and **8** were slightly lower than that of the unmodified one because the K_m values of

Table 2: Kinetic Parameters for the RNA Substrate Cleavage Reactions by the Unmodified and Mutant Deoxyribozymes in the Presence of Mg^{2+} [a]

deoxyribozyme	substitution	K_m (nM)	k_{cat} ($\times 10$ min^{-1})	k_{cat}/K_m ($\times 10^{-5}$ M^{-1} min^{-1})
unmodified[b]	none	291 ± 2.3	2.09 ± 0.78	7.2
mutant **19**	$G_1 \rightarrow$ 7-deaza-dG	560 ± 49	1.87 ± 0.16	3.3
mutant **20**	$G_1 \rightarrow$ 2-aminopurine	827 ± 51	1.92 ± 0.18	2.3
mutant **21**	$G_2 \rightarrow$ 7-deaza-dG	283 ± 19	2.16 ± 0.19	7.6
mutant **22**	$G_2 \rightarrow$ 2-aminopurine	778 ± 41	2.28 ± 0.20	2.9
mutant **23**	$G_{10} \rightarrow$ 7-deaza-dG	298 ± 22	2.10 ± 0.17	7.1
mutant **24**	$G_{10} \rightarrow$ 2-aminopurine	304 ± 27	0.614 ± 0.060	2.0

[a] All experiments were carried out in a buffer containing 50 mM Tris-HCl (pH 8.0) and 25 mM Mg^{2+} under multiple-turnover conditions with 10−1000 nM 5′-end ^{32}P-labeled RNA substrate and 1 nM deoxyribozyme at 37 °C. [b] Data from ref *24*.

mutants **7** and **8** were 2.0 and 2.4 times that of the unmodified one, respectively. These results indicated that N2 with A_7 and A_8 might exert a weak inhibition during the folding step.

dG Substitution. In the *Tetrahymena* group I intron and the hammerhead ribozyme, N7 and O6 of G are known to play specific roles in active domain folding and metal ion binding (*40*, *41*). To determine the specific role of dG in our catalytic loop, RNA cleavage reactions were carried out with mutants **10**−**12**, which have G_1, G_2, or G_{10} substituted with dI (Figure 2g,h). The results of the RNA cleavage reactions by mutants **10**−**12** in the presence of 25 mM Ca^{2+} (pH 8.0) at 37 °C showed that the RNA cleavage yields by these mutants were the same as that for the unmodified one (see Figure S4 of the Supporting Information). The k_{cat}/K_m values of mutants **10**−**12** were also similar to that of the unmodified one (see Table 1). These results suggested that N2 of G_1, G_2, and G_{10} has little influence on the RNA cleavage activity.

The RNA cleavage reactions were also carried out with mutants **13**−**18**, which have G_1, G_2, and G_{10} substituted with 7-deaza-dG or 2-aminopurine (Figure 2g,i,j). Whereas the k_{cat}/K_m values of mutants **14** and **15** were very similar to that for the unmodified one, those for mutants **13** and **16**−**18** were much lower. This decrease in the k_{cat}/K_m values for mutants **13**, **16**, and **17** depended on the K_m value, and that of mutant **18** depended on the k_{cat} value. The K_m values of mutants **13**, **16**, and **17** were ∼4.5, ∼6.7, and ∼6.3 times that of the unmodified one, respectively. The k_{cat} value of mutant **10** was 0.025 times that of the unmodified one. Therefore, the results indicate that N7 and O6 of G_1 and O6 of G_2 contributed to the folding of the deoxyribozyme−RNA substrate complex and that O6 of G_{10} influenced its RNA cleavage activity.

Effect of Ca^{2+} and Mg^{2+} on Deoxyribozyme Reactions. The catalytic efficiency of the unmodified form was much higher in the presence of Ca^{2+} than in the presence of Mg^{2+} (*24*, *25*). To determine the difference in the functional group in the presence of Ca^{2+} or Mg^{2+}, RNA cleavage reactions with mutants **19**−**24** were carried out in the presence of 25 mM Mg^{2+} (pH 8.0) at 37 °C. Table 2 lists the kinetic parameters of these deoxyribozyme reactions. Whereas the k_{cat}/K_m values of mutants **21** and **23** were very similar to that of the unmodified one, the k_{cat}/K_m values of mutants **19**, **20**, **22**, and **24** were much lower. This decrease in the k_{cat}/K_m values of mutants **19**, **20**, and **22** depended on the K_m value, and that of mutant **24** depended on the k_{cat} value.

To investigate the different roles of Ca^{2+} and Mg^{2+}, RNA cleavage reactions were carried out at various ratios of Ca^{2+} and Mg^{2+} (see Figure 4). The minimum K_m value was obtained at 25 mM Ca^{2+} and 0 mM Mg^{2+}, suggesting that Ca^{2+} was a better metal ion for K_m than Mg^{2+}. The maximum k_{cat} value was found at 12.5 mM Ca^{2+} and 12.5 mM Mg^{2+}, although it was only ∼1.3 times that at 25 mM Ca^{2+}. The k_{cat} value at 25 mM Ca^{2+} was 10 times that at 25 mM Mg^{2+}. These results indicate that Ca^{2+} has a greater influence on k_{cat} than Mg^{2+} as well as on K_m.

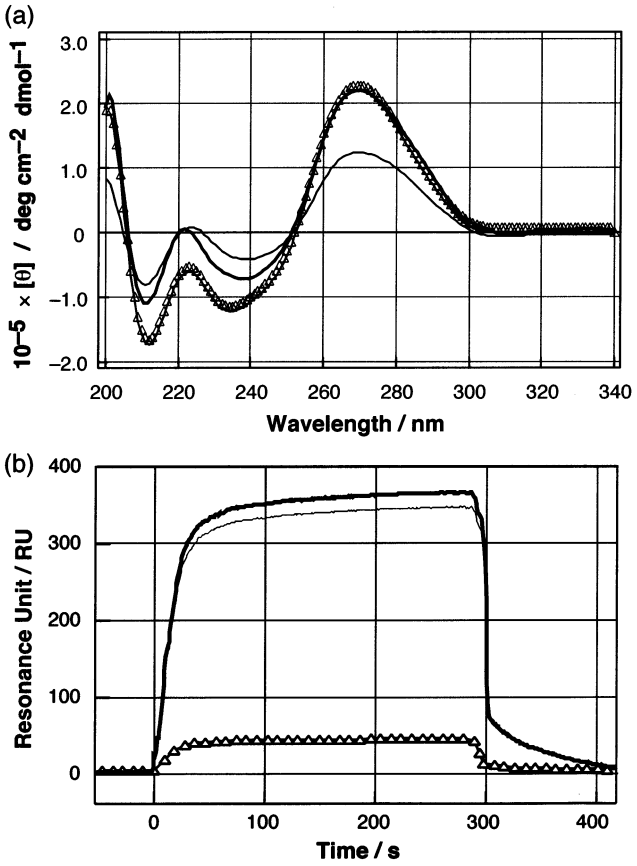

FIGURE 3: (a) Typical CD spectra of the complexes of the unmodified (thick line), mutant **17** (△), mutant **18** (thin line), and pseudo-RNA substrate [rAGGGAG(dA)UGCCAGGC] at 5 °C. The total concentration of the sample was 10 μM. (b) Typical SPR sensorgrams of the binding of the unmodified (thick line), mutant **17** (△), and mutant **18** (thin line) to the immobilized pseudo-RNA substrate [rAGGGAC(dA)UGCCAGGC] at 20 °C. The deoxyribozyme concentration was 2.0 μM. All experiments were carried out in a buffer containing 50 mM Tris-HCl (pH 8.0) and 25 mM Ca^{2+}.

Formation of a Complex between the Deoxyribozyme and Its RNA Substrate. The pH dependency of k_{cat} with the unmodified one showed that k_{cat} reflected its RNA cleavage

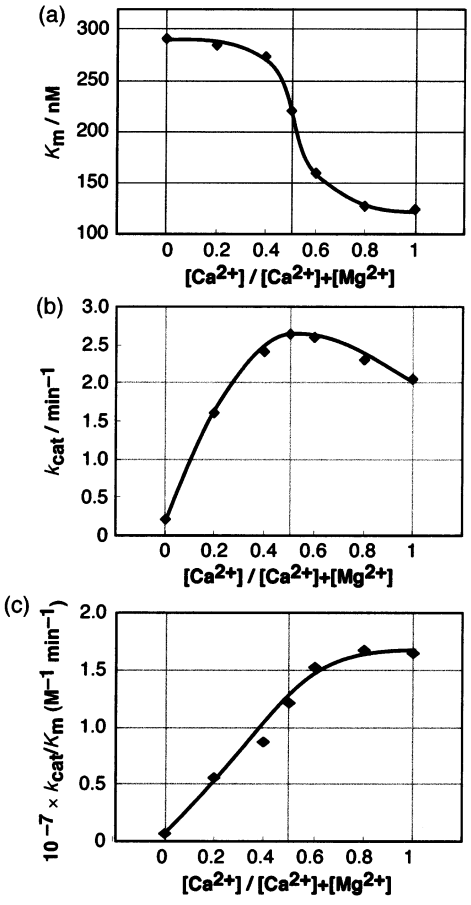

FIGURE 4: Plots of (a) K_m, (b) k_{cat}, and (c) k_{cat}/K_m vs the concentration ratio of Ca^{2+} with Mg^{2+} on the unmodified deoxyribozyme reactions. The total concentration of Ca^{2+} and Mg^{2+} was 25 mM. All experiments were carried out in a buffer with 50 mM Tris-HCl (pH 8.0) at 37 °C.

activity, as described above. In the case of K_m, it was unclear whether K_m for the deoxyribozyme corresponded to a constant for binding of the deoxyribozyme to its RNA substrate. To investigate the binding between the deoxyribozyme and its RNA substrate, the UV melting, CD, and SPR data were measured in the presence of 25 mM Ca^{2+} (pH 8.0). Table 1 lists the T_m values of the formation of the complex of the deoxyribozyme and its pseudo-RNA substrate. Interestingly, a comparison between the K_m and T_m values is consistent with the K_m values and reflected the stability of the deoxyribozyme−RNA substrate complexes.

Figure 3a shows the typical CD spectra of the complexes of the unmodified form, mutant **17** or **18**, and the pseudo-RNA substrate. These CD spectra show a positive peak around 270 nm and a relatively weak negative peak around 240 nm, indicating a normal A-like structure (*42*). As shown in Figure 3a, although the peak intensity around 270 nm for mutant **17** was very similar to that of the unmodified form, the peak of mutant **18** was much smaller. The order in the peak intensity at 270 nm was in agreement with that of the relative K_m values. These results indicate that the structural formation difference between the active and inactive forms was due to the overall geometry of the complexes in the presence of Ca^{2+}.

To further clarify the kinetic properties of this binding between the deoxyribozyme and its RNA substrate, the binding kinetics were measured with the SPR apparatus at 20 °C. Figure 3b shows the typical SPR sensorgrams for the unmodified form and mutants **17** and **18** flowing over the immobilized pseudo-RNA substrate. When the deoxyribozyme binds to the ligand immobilized on the sensor chip, the RU value increased due to changes in the refractive index as shown by the RU in real time. Binding of the deoxyribozyme to the immobilized ligand was characterized by a single-step process with rapid association and dissociation, since kinetic traces did not exhibit two phases as is the case with the binding of a substrate to that of the *Tetrahymena* group I intron (*43*). When the unmodified form and mutant **18** were passed over the sensor chip coated with the immobilized probe, a high resonance (350 RU) was registered, but with mutant **17**, a value of only 40 RU was obtained. To further clarify the effect of the association and dissociation processes between the deoxyribozyme and its RNA substrate, kinetic parameters k_a, k_d, and $\Delta G°_{20}$ are listed

Table 3: Kinetic Parameters for the Binding of the Unmodified or Mutant Deoxyribozymes to the Immobilized Pseudo-RNA Substrate [rAGGGAC(dA)UGCCAGGC][a]

deoxyribozyme	substitution	k_a ($\times 10^{-4}$ M^{-1} s^{-1})	k_d ($\times 10^{2}$ s^{-1})	$\Delta G°_{20}$ [b] (kcal/mol)
unmodified[c]	none	5.62 ± 0.48	5.38 ± 0.73	−8.1
mutant **1**	C_6 → d^pC	4.96 ± 0.44	5.49 ± 0.69	−8.0
mutant **2**	C_9 → dm^5C	5.34 ± 0.44	7.25 ± 0.66	−7.9
mutant **3**	C_9 → d^pC	9.87 ± 0.87	1.87 ± 0.10	−9.0
mutant **4**	A_7 → 7-deaza-dA	5.01 ± 0.48	7.60 ± 0.55	−7.8
mutant **5**	A_8 → 7-deaza-dA	5.00 ± 0.49	7.32 ± 0.68	−7.8
mutant **6**	A_{11} → 7-deaza-dA	5.47 ± 0.47	7.01 ± 0.58	−7.9
mutant **7**	A_7 → 2-amino-dA	3.23 ± 0.24	13.3 ± 1.2	−7.2
mutant **8**	A_8 → 2-amino-dA	3.00 ± 0.26	14.7 ± 1.3	−7.1
mutant **9**	A_{11} → 2-amino-dA	5.64 ± 0.50	7.21 ± 0.52	−7.9
mutant **10**	G_1 → dI	5.13 ± 0.39	7.77 ± 0.64	−7.8
mutant **11**	G_2 → dI	4.99 ± 0.41	7.10 ± 0.58	−7.8
mutant **12**	G_{10} → dI	5.51 ± 0.41	6.99 ± 0.57	−7.9
mutant **13**	G_1 → 7-deaza-dG	0.957 ± 0.092	39.4 ± 1.1	−5.9
mutant **14**	G_2 → 7-deaza-dG	5.14 ± 0.42	7.49 ± 0.70	−7.8
mutant **15**	G_{10} → 7-deaza-dG	5.47 ± 0.48	7.10 ± 0.59	−7.9
mutant **16**	G_1 → 2-aminopurine	2.33 ± 0.28	28.8 ± 1.5	−6.6
mutant **17**	G_2 → 2-aminopurine	1.13 ± 0.11	37.9 ± 2.5	−6.0
mutant **18**	G_{10} → 2-aminopurine	4.81 ± 0.35	8.24 ± 0.77	−7.7

[a] All experiments were carried out in a buffer containing 50 mM Tris-HCl (pH 8.0) and 25 mM Ca^{2+} at 20 °C. [b] The $\Delta G°_{20}$ value was calculated from eq 3. [c] Data from ref *25*.

in Table 3. The $\Delta G°_{20}$ value of the unmodified form was similar to those of mutants **1**, **2**, **4**−**6**, **9**−**12**, **14**, **15**, and **18**, whereas the $\Delta G°_{20}$ values of mutants **7**, **8**, **13**, **16**, and **17** were greater than that of the unmodified form by more than 1 kcal/mol. The $\Delta G°_{20}$ value for mutant **3** was smaller than that of the unmodified one. These results will be discussed in comparison with the kinetics for the RNA cleavage reactions.

DISCUSSION

G·A Mismatched Base Pairs. The metal ion binding sites within ribozymes and deoxyribozymes can be identified using unnatural nucleotides. dI, which does not have the 2-NH_2 group of dG, is a good probe for structure-specific minor groove interactions with amino groups of dG (*44*−*46*). 2-Aminopurine and 7-deaza-dG are useful for probing for the presence of the Hoogsteen interaction, chelation sites for metal ions, and nucleic acid−protein interactions (*45*−*48*). Taira et al. investigated various DNA enzymes with nucleotide substitutions (G → A or A → G) in the catalytic loop, suggesting that the catalytic activity depends on one base in the catalytic loop (*49*). Many X-ray and NMR studies have indicated that metal ions are directly bound near the non-Watson−Crick base pairs. G·A base pairs are commonly found in the secondary structural motifs of biological molecules, including the hammerhead ribozyme and the *Tetrahymena* group I intron (*40*, *41*). The appendant atoms of the mismatches afford tertiary interactions, serve as recognition sites for protein, and also stabilize three-dimensional structures. These functions may be achieved by different conformations of the G·A base pairs. The G·A mismatches were specific structures, because these structures have roles as metal ion binding sites or undergo interactions between receptors and acceptors (*50*). These results suggested that the folding of the mismatch regions would be at the Ca^{2+} binding sites.

The X-ray crystallographic and NMR studies of the structures of duplex DNA and RNA showed four possible G·A base pair conformations: G(*anti*)·A(*syn*), sheared G·A, G(*syn*)·A^+(*anti*), and G(*anti*)·A(*anti*) (Figure 2k−n, respectively) (*51*). The precise form of the mismatched base pairs depended on the pH, salt concentration, and, in particular, the sequence environment. In this study, first, the results of RNA cleavage reactions by mutants **4**−**6** had no influence on the catalytic activity. Thus, the G(*anti*)·A(*syn*) base pair with two hydrogen bonds, O6(G)−N2(A) and N1(G)−N7(A), might not form in the catalytic loop. Second, the results of the RNA cleavage reactions by mutants **10**−**12** had no influence on the catalytic activity. Thus, the sheared G·A base pair with two hydrogen bonds, N2(G)−N7(A) and N3(G)−N2(A), might not form in the catalytic loop. Third, the formation of the G(*syn*)·A^+(*anti*) base pair with two hydrogen bonds, O6(G)−N2(A) and N7(G)−$N1^+$(A), requires the protonation of N1 of dA. The pK_a value of N1 of dA is 3.5 (*51*), and the RNA cleavage condition was pH 8.0, suggesting that this mismatched base pair might not form. These results suggest that the G(*anti*)·A(*anti*) conformations of the G_1·A_8 and G_2·A_7 mismatched base pairs would form in the catalytic loop.

Modification in the Catalytic Loop of the Deoxyribozyme To Obtain High Catalytic Activity. As a site for molecular reporter devices for oligodeoxyribonucleotides, the carbon 5 position of the pyrimidine nucleotide is nearly ideal, because groups of different sizes may be attached without adversely affecting duplex formation (*37*). In addition, each methyl group attached to uracil in either RNA or DNA adds 0.1−0.5 kcal/mol of stability to the double- and triple-helical structures (*52*). It is thought that this effect is due to the increased polarizability of the methylated bases, which enhances the van der Waals interactions with the neighboring bases (*53*).

Freier and Altmann investigated the ΔT_m values of RNA−DNA hybrids containing substitutions at the carbon 5 position of dC (*37*). Because functional groups of differing size may be attached without an adverse effect on the formation of the RNA−DNA hybrid, the carbon 5 position of the pyrimidine nucleotide is promising for hybrids (*54*). The 8 bp RNA−DNA rGCCGUGAG−dCTCACGG**X** hybrid, which has **X** substituted with d^PC, was more stable than the rGCCGUGAG−dCTCACGG**C** hybrid (data not shown). This indicated that the RNA−DNA hybrid allows stacking of the propynyl group of the base on the 5′-side of the junction onto the 3′-adjacent base. This stabilizing effect of d^PC leads to the high cleavage activity of the deoxyribozyme. In fact, our results indicated that the catalytic activity of mutant **3**, which has C_9 substituted with d^PC, was the best of all the mutants and was much higher than that of the unmodified one. Thus, substituting d^PC for dC in the catalytic loop of the ribozymes and deoxyribozymes would be one of the best strategies for increasing the catalytic activity.

Conclusion. The catalytic activity of the small Ca^{2+}-dependent deoxyribozyme depends on the functional groups of the nucleobases in the catalytic loop of the deoxyribozyme−RNA substrate complex. In this study, to clarify the factors that contribute to the efficient catalytic activity of the deoxyribozyme, RNA cleavage reactions were carried out using 24 mutant variant deoxyribozymes containing one unnatural DNA nucleotide, i.e., 7-deaza-dG, d^PC, etc. We proposed that two G_1·A_8 and G_2·A_7 mismatched base pairs may be formed in the catalytic loop of this deoxyribozyme. Our results suggest that the deoxyribozyme−RNA substrate complex has Ca^{2+} binding sites that produce an efficient RNA cleavage reaction and formation of an active conformation and that substituting d^PC for dC in the catalytic loop would be one of the best strategies for increasing the catalytic activity of the deoxyribozyme.

ACKNOWLEDGMENT

We acknowledge Mr. Daisuke Miyoshi (Konan University) for critically reading the manuscript and helpful comments.

SUPPORTING INFORMATION AVAILABLE

Text describing the detailed results of the catalytic activity for the unmodified versus [Ca^{2+}] plots, a log(k_{cat}) versus pH plot on the unmodified reactions, RNA cleavages by the mutant deoxyribozymes that have dAs substituted with 7-deaza-dA or 2-amino-dA, RNA cleavages by the mutant deoxyribozymes that have dGs substituted with dI, 7-deaza-dG, or 2-aminopurine, and plot of the catalytic activity for the unmodified form versus the concentration ratio of Ca^{2+} and Mg^{2+}. This material is available free of charge via the Internet at http://pubs.acs.org.

REFERENCES

1. Treiber, D. K., and Williamson, J. R. (1999) *Curr. Opin. Struct. Biol. 9*, 339−345.
2. Treiber, D. K., Rook, M. S., Zarrinkar, P. P., and Williamson, J. R. (1998) *Science 279*, 1943−1946.
3. Walter, N. G., Burke, J. M., and Millar, D. P. (1999) *Nat. Struct. Biol. 6*, 544−549.
4. Welch, P. J., Barber, J. R., and Wong-Staal, F. (1998) *Curr. Opin. Biotechnol. 9*, 486−496.
5. Pyle, A. M. (1993) *Science 261*, 709−714.
6. Grosshans, C. A., and Cech, T. R. (1989) *Biochemistry 28*, 6888−6894.
7. Tsang, J., and Joyce, G. F. (1996) *J. Mol. Biol. 262*, 31−42.
8. Komatsu, Y., Kanzaki, I., Shirai, M., and Ohtsuka, E. (1997) *Biochemistry 36*, 9935−9940.
9. Sood, V. D., Beattie, T. L., and Collins, R. A. (1998) *J. Mol. Biol. 282*, 741−750.
10. Wang, S., Karbstein, K., Peracchi, A., Beigelman, L., and Herschlag, D. (1999) *Biochemistry 38*, 14363−14378.
11. Nakano, S., Chadalavada, D. M., and Bevilacqua, P. C. (1999) *Science 287*, 1493−1497.
12. Disney, M. D., Testa, S. M., and Turner, D. H. (2000) *Biochemistry 39*, 6991−7000.
13. Ohmichi, T., Okumoto, Y., and Sugimoto, N. (1998) *Nucleic Acids Res. 26*, 5655−5661.
14. Dahm, S. C., Derrick, W. B., and Uhlenbeck, O. C. (1993) *Biochemistry 32*, 13040−13045.
15. McConnell, T. S., Herschlag, D., and Cech, T. R. (1997) *Biochemistry 36*, 8293−8303.
16. Nesbitt, S. M., Erlacher, H. A., and Fedor, M. J. (1999) *J. Mol. Biol. 286*, 1009−1024.
17. Murray, J. B., Seyhan, A. A., Walter, N. G., Burke, J. M., and Scott, W. G. (1998) *Chem. Biol. 5*, 587−595.
18. Curtis, E. A., and Bartel, D. P. (2001) *RNA 7*, 546−552.
19. Santoro, S. W., and Joyce, G. F. (1997) *Proc. Natl. Acad. Sci. U.S.A. 94*, 4262−4266.
20. Faulhammer, D., and Famulok, M. (1996) *Angew. Chem., Int. Ed. Engl. 35*, 2873−2841.
21. Carmi, N., Shulta, L. A., and Breaker, R. R. (1996) *Chem. Biol. 3*, 1039−1046.
22. Breaker, R. R., and Joyce, G. F. (1994) *Chem. Biol. 1*, 223−229.
23. Li, J., Zheng, W., Kwonm, A. H., and Li, Y. (2000) *Nucleic Acids Res. 28*, 481−488.
24. Sugimoto, N., Okumoto, Y., and Ohmichi, T. (1999) *J. Chem. Soc., Perkin Trans. 2*, 1382−1388.
25. Okumoto, Y., and Sugimoto, N. (2000) *J. Inorg. Biochem. 82*, 189−195.
26. Santoro, S. W., and Joyce, G. F. (1998) *Biochemistry 37*, 13330−13342.
27. Kuwabara, T., Warashina, M., Tanabe, T., Tani, K., Asano, S., and Taira, K. (1997) *Nucleic Acids Res. 25*, 3074−3081.
28. Okumoto, Y., Ohmichi, T., and Sugimoto, N. (2002) *Biochemistry 41*, 2769−2773.
29. Kierzek, R., Caruthers, M. H., Longfellow, C. E., Swinton, D., Turner, D. H., and Freier, S. M. (1986) *Biochemistry 25*, 7840−7846.
30. Richards, E. G. (1975) in *Handbook of Biochemistry and Molecular Biology: Nucleic Acids* (Fasman, G. D., Ed.) Vol. 1, pp 597, CRC Press, Cleveland, OH.
31. Hendry, P., McCall, M. J., and Lockett, T. J. (1997) in *Methods in Molecular Biology* (Turner, P. C., Ed.) Vol. 74, pp 221−229, Humana Press Inc., Totowa, NJ.
32. Sugimoto, N., Nakano, S., Katoh, M., Nakamuta, H., Ohmichi, T., Yoneyama, M., and Sasaki, M. (1995) *Biochemistry 34*, 11211−11216.
33. Bondeson, K., Frostell-Karlsson, Å., Fagerstam, L., and Magnusson, G. (1993) *Anal. Biochem. 214*, 245−251.
34. O'Shannessy, D. L., Brigham-Burke, M., Soneson, K. K., Hensley, P., and Brooks, I. (1993) *Anal. Biochem. 212*, 457−468.
35. Uebayashi, M., Uchimaru, T., Kokuma, T., Sawata, S., Shimayama, T., and Taira, K. (1994) *J. Org. Chem. 59*, 7414−7420.
36. Warashina, M., Takagi, Y., Sawata, S., Zhou, D., Kuwabara, T., and Taira, K. (1997) *J. Org. Chem. 62*, 9138−9147.
37. Freier, S. M., and Altmann, K.-H. (1997) *Nucleic Acids Res. 25*, 4429−4443.
38. Sugimoto, N., Yoneyama, M., and Sasaki, M. (1995) *Rep. Prog. Polym. Phys. Jpn. 38*, 695−698.
39. Fu, D. J., and McLaughlin, L. W. (1992) *Biochemistry 31*, 10941−10945.
40. Scott, W. G., Murray, J. B., Arnold, J. R. P., Stoddard, B. L., and Klug, A. (1996) *Science 274*, 2065−2069.
41. Cate, J. H., Hanna, R. L., and Doudna, J. A. (1997) *Nat. Struct. Biol. 4*, 553−558.
42. Johnson, W. C., Jr. (1996) in *Circular Dichroism and the Conformational Analysis of Biomolecules* (Fasman, G. D., Ed.) pp 433−468, Plenum Press, New York.
43. Bevilacqua, P. C., Kierzek, R., Johnoson, K. A., and Turner, D. H. (1992) *Science 258*, 1335−1358.
44. Musier-Forsyth, K., Usman, N., Scaringe, S., Doudna, J., Green, R., and Schimmel, P. (1991) *Science 253*, 784−786.
45. Iwai, S., Pritchard, C. E., Mann, D. A., Karn, J., and Gait, M. J. (1992) *Nucleic Acids Res. 20*, 6465−6472.
46. Hamy, F., Asseline, U., Grasby, J. A., Iwai, S., Pritchaed, C. E., Silm, G., Butler, P. J. G., Karn, J., and Gait, M. J. (1993) *J. Mol. Biol. 230*, 111−123.
47. Doudna, J. A., Szostak, J. W., Rich, A., and Usman, N. (1990) *J. Org. Chem. 55*, 5547−5549.
48. SantaLucia, J., Jr., Kierzek, R., and Turner, D. H. (1991) *J. Am. Chem. Soc. 113*, 4313−4322.
49. Warashina, M., Kuwabara, T., Nakamatsu, Y., and Taira, K. (1999) *Chem. Biol. 6*, 237−250.
50. Abramovitz, D. D., and Pyle, A. M. (1997) *J. Mol. Biol. 266*, 493−506.
51. Brown, T., and Hunter, W. N. (1997) *Biopolymers 44*, 91−103.
52. Xodo, L. E., Manzini, G., Quadrifoglio, F., van der Marel, G. A., and van Boom, J. H. (1991) *Nucleic Acids Res. 12*, 5625−5631.
53. Sowers, L. C., Shaw, B. S., and Sedwick, W. D. (1987) *Biochem. Biophys. Res. Commun. 148*, 790−794.
54. Barnes, T. W., III, and Turner, D. H. (2001) *J. Am. Chem. Soc. 123*, 9186−9187.

BI020364Z